N. Lior, P. S. Ayyaswamy, J. O'Leary, K. Kauffman, H. Yeh and H. G. Lorsch, "Thermal Energy Storage Considerations for Solar Thermal Power Generation," Proceedings of the 11th Intersociety Energy Conversion Engineering Conference, paper No. 769107, State Line, NV, September 12 17, pp. 613 622, 1976.

THERMAL ENERGY STORAGE CONSIDERATIONS FOR SOLAR-THERMAL POWER GENERATION

N. Lior, P. S. Ayyaswamy, J. O'Leary, K. W. Kauffman, H. Yeh
University of Pennsylvania
Philadelphia, Pennsylvania 19174

H. G. Lorsch
Franklin Institute Research Laboratories
Philadelphia, Pennsylvania 19103

Abstract

The problem of thermal energy storage for solar-thermal power generation is examined. Major conceptual systems for thermal storage are proposed and described. Storage modes through sensible heat, latent heat (phase change), and thermochemical energy are reviewed and proposed. A survey of applicable materials for thermal storage, which includes available thermophysical properties, compatibility with containing and heat transfer interfaces, and economics, is presented. The energy storage related parameters (such as temperatures, heat fluxes and quantities) of two major conceptual systems for solar-thermal power generation are identified for a power station size of 100MWe. Mathematical details relevant to transient analyses of thermal storage have been developed and discussed.

NOMENCLATURE

A : cross-sectional area
B : Biot number
C : specific heat
d : half-thickness of slab
D : diameter of storage pellets
G : half of gap between slabs; mass flux of fluid
H : parameter defined in equation 15; height
h : heat transfer coefficient
h_{fg} : latent heat of vaporization of fluid
k : thermal conductivity
L : length of storage bed
$\dot{m}$: mass flow rate of fluid
N : number of zones in storage bed; number of half-slabs
ΔP : pressure drop
S : Stefan number
T : temperature
t : time
U : overall heat transfer coefficient
v : velocity
x : coordinate in flow direction
$\hat{x}$: quality
Y : width of slab
z : direction through slab

Greek Symbols

α : thermal diffusivity
γ : parameter defined in equation 15
ε : void fraction
η : nondimensional z coordinate
θ : nondimensional temperature
λ : latent heat of phase change material
μ : viscosity of fluid
ξ : nondimensional x coordinate
ρ : density
τ : time (nondimensional)

Superscripts
* : interface location

Subscripts
M : melting condition
f : fluid property
i : inlet condition; zone
ℓ : local value
b : storage material property

INTRODUCTION

There exists a growing interest in solar-thermal power generation. Most of the proposed system concepts involve the utilization of solar energy to generate steam or heat gas, which drive a prime mover in a Rankine or Brayton cycle, respectively. In addition to the problems of solar energy collection and concentration (when applicable), one of the major and most complex elements of solar power generation is that of energy storage. Due to the intermittency of solar radiation, if economical and steady power generation capacity is deisred, it is necessary to incorporate energy storage into the system. The storage would be charged when insolation is adequate, and discharged when insolation is inadequate or absent. The charging process would normally be accomplished simultaneously with power production, by directing a part of the total solar energy collected to the storage system and another part to the prime mover.

A variety of energy storage concepts are possible and being considered for this application. One of the concepts uses mechanical storage, most likely to be accomplished by pumping water to an elevated basin during the charging period and releasing it to flow downward through turbines during discharge [1], or by compressing and subsequently releasing the compressed air or by storage in special flywheels [2]. Other systems involve the storage of energy in electrical batteries, the production of fuels such as hydrogen and methanol and the storage of these fuels, and the storage of the solar-thermal energy by several means, using the stored energy as the heat source for the normal power cycle fluid. Thermal storage appears to be at present one of the most promising concepts, both due to the fact that it allows a smaller turbogenerator plant and because it reduces the severe transients associated with the part-time operation of the thermal cycle in various mechanical or electrical storage systems [3]. This paper treats thermal storage only, and specifically dwells on the materials and heat transfer aspects.

TYPICAL CONCEPTUAL SOLAR-THERMAL POWER CYCLES

Since the first experiments by Mouchot and by Ericsson, which started in about 1870, several solar-thermal power plants were built and tested, mostly by concentrating solar energy with a conical, or paraboloidal dish mirror concentrator, or with a parabolical trough concentrator [4]. These systems were few and relatively small. The renewed interest in solar-thermal power generation during the past few years has resulted in studies of several concepts, some essentially applying modern technology to the systems tested in the past, and some entirely new.

The systems under consideration can be classified into nonconcentrating and concentrating types, the former resulting in working fluid temperatures of 150°C at most and the latter essentially limited by material considerations, with typical recommended temperatures of about 500°C for steam and about 800-1100°C for gas (such as helium or air).

Nonconcentrating, low temperature concepts utilize either flat plate solar collectors (preferably vacuum-insulated) [5] or solar ponds which either use a salt concentration gradient [6], or insulating plastic covers at the water surface [7] to minimize heat losses. Special flat plate collectors may produce fluid temperatures of up to 150°C, and the solar ponds would operate at 90°C at most. Whereas the low temperatures produce relatively low overall system efficiencies (less than 4%), the systems are less complex and thus presumably less costly than the concentrating ones. They can also use the diffuse component of solar radiation, which the concentrating systems do not.

The high temperature concentrating concepts can be classified into two groups: the distributed collector concepts where fluid is heated in each separate receiver and is pumped to a central prime mover [8], or a central collector concept, where a large number of flat heliostatic mirrors reflect sunlight to a central receiver located on a high tower, where it heats the fluid. The hot fluid is transported to the central prime mover located on the ground [3, 8-10]. Specifically, the distributed collector system described in [8] uses a parabolical trough line-focusing collector to heat fluid to a temperature of about 300°C, whereas the central collector system is planned for fluid temperatures between 500°C and 1100°C. Most of the recent studies concur [11] that for power plant sizes above 100 MWe, the most economical system is the central collector system, using superheated steam at about 500°C and 8.6 to 15.9 MN/m^2 (1250 to 2300 psia).

A typical power cycle schematic is shown in Fig. 1. This paper will concentrate on the thermal storage aspects of such a cycle.

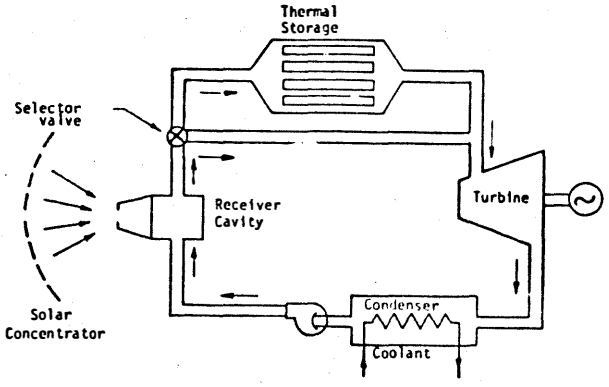

Figure 1. Schematic of a Solar-Thermal Power Cycle

THERMAL STORAGE CONCEPTS APPLICABLE TO SOLAR-THERMAL POWER CYCLES

The major concepts under consideration for this purpose are:

1. Sensible Heat Storage. Here the thermal storag material is heated by the working fluid, gaining temperature and thermal energy. The storage material which is usually a solid, but sometimes a liquid, does not change phase during the charging (heating) or discharging (cooling) period. Solids such as rock, iron, salts and others have been considered, and typical liquids are water, oil, or some other special organic liquids. The heat transfer and design aspects are fairly straightforward and can generally be handled by state-of-the-art engineering. The materials to be used are also commonplace, and relatively inexpensive. The major disadvantage of this system is the relatively low specific heat of most materials, requiring either a very large temperature swing for a practical amount of storage material, which is rather undesirable for prime mover operation, or requires a very large quantity of storage material for smaller temperature swings. Typical sizes for a 100 MWe solar-thermal plant are shown below.

An attractive application of sensible heat storage is through the utilization of a "steam accumulator", which is fairly common in Europe [12]. While several versions of the system are in existence, it essentially utilizes steam to heat water by direct contact condensation, and steam is discharged from the accumulator when needed by slight pressure reduction and flashing. One important advantage of this system is that it uses the same fluid (water) for the power cycle and the thermal storage. A technical and economical study of this system was performed [13] showing it to be less expensive than a stratified hot water displacement storage tank.

2. Phase Change Thermal Storage. Storing and recovering heat through the phase change process is advantageous due to the fact that the latent heat of most materials is much higher than their specific heat, thus requiring a much smaller amount of storage material. Furthermore, the thermal storage process occurs at a constant temperature, which is highly desirable for the operation of the prime mover (during the discharge period). Latent heat storage could be implemented either through solid-liquid phase change or through liquid-vapor phase change. In both cases the heat transfer and design aspects are much more complex than those in the sensible heat case. Furthermore, although liquid-vapor phase change has a higher latent heat, it is

associated with very high pressures and volume changes, introducing severe containment difficulties, and is therefore normally not too applicable. Most of the phase change thermal storage schemes under consideration incorporate the solid-liquid transformation [8, 14-19] and will also be treated here.

3. Thermochemical Storage. Some of the major methods considered under this category include the generation of hydrogen from metal hydrides [20], heat of hydration of certain metallic oxides [21], and the utilization of liquid-vapor phase change latent heat with the subsequent absorption of the vapor in a second liquid (this is somewhat similar to part of the process in the absorption refrigeration), thus eliminating the severe problem of storing the large volume of vapor, mentioned earlier above [22,23]. These systems seem to be promising, but are now still at a relatively early stage of development.

PHASE CHANGE MATERIALS FOR THERMAL STORAGE

The material properties important to thermal storage have been discussed in detail elsewhere [24]. Materials must melt congruently, have high heats of fusion, nucleate solid phase from the liquid without supercooling below the melting temperature, be chemically stable, and be readily available in quantity at reasonable cost. The cost of using a particular material also depends upon the container/heat exchanger surface area requirement, the corrosivity of the material, the volume change on freezing, and any special requirements for preparation and handling. These cost factors are considered below for inorganic salts and alloys.

Volume changes for materials which expand on fusion can be accommodated in closed containers at the cost of increasing the container area, provided neither the volume change nor the volume of the container is large. A 10% decrease in volume on freezing of the material in a horizontal cylinder results in a 25% decrease in effective heat transfer surface if the void volume is located at the top of the cylinder. More heat transfer must therefore be provided to make up for this loss in order to maintain the desired heat transfer rate. The void volume may also be dispersed throughout the heat storage material depending on the rate of freezing, the viscosity of the liquid, and the surface tensions among the materials. Where small voids are formed, the effect of volume change is to decrease the overall thermal conductivity of the material. In either case, additional surface must be provided to maintain the needed rate of heat transfer. Volume changes for some inorganic salts and metals are presented in Table I. Data which are less reliable are shown in parentheses. Except for calcium and barium chlorides and sodium and potassium nitrates, the salts listed have larger volume changes than the metals.

Table I. Volume Changes on Fusion

Material	Volume Change on Fusion, %	Material	Volume Change on Fusion, %
$AlCl_3$	86.3	NaCl	25.0
$BaCl_2$	3.5	NaF	21.7 (27.4)
$CaCl_2$	(0.9)	$NaNO_3$	9.7
LiCl	26.2	Al	5.2
LiF	22.9 (29.4)	Fe	-6.7
$LiNO_3$	17.6	Pb	3.9
KCl	17.3	Sn	2.6
KF	14.7 (17.2)	Zn	7.5
KNO_3	3.1		

Corrosion and preparation may be problems for some of the salts. Nitrates tend to passivate iron, but acidic chloride salts such as $CaCl_2$ are known to break down passive films and stimulate corrosion. These may require more expensive containment/heat transfer surfaces. The presence of small amounts of water must be avoided, and salts which are even slightly hygroscopic, such as sodium and potassium nitrates and potassium and calcium chlorides, must be prepared and handled carefully to avoid atmospheric moisture. Corrosion and preparation are less of a problem for the alloys, although care must be taken in selecting the containment/heat transfer surface to avoid unwanted alloying.

Thermal conductivity and volumetric storage density (MJ/m^2) are at least as important as raw material cost in determining the overall cost of thermal storage [19]. This is because of the cost of providing the containment/heat transfer surface. Relevant data for some of the least expensive and best performing salts and alloys are given in Table II.

Heat exchanger surface areas were calculated on the basis of a 14°C temperature difference and a 12-hour discharge time for the storage device. A cost of $\$53.8/m^2$ of heat exchanger surface was assumed. The total costs in the right hand column comprise the costs of the storage raw material and of the heat exchanger surfaces. The cost of installing them inside the storage container, as well as the cost of the container itself, were not included.

As can be seen from Table II, the advantage of low raw materials cost for the salts is largely counterbalanced by the requirements for large, expensive heat exchanger surfaces due to their low conductivities. While the raw materials cost is higher for the alloys, as a group they produce lower cost heat storage devices than do the salts. If the containment cost is also considered, the alloys show up even more favorably than the salts because of their greater volumetric heat storage density.

HEAT TRANSFER AND SIZING OF THERMAL STORAGE SYSTEMS

As indicated earlier, two of the distinct and major concepts of thermal storage applicable to solar-thermal power cycles are the sensible heat system and the phase change system. The particular nature of the heat storage system determines the heat transfer aspects and the ultimate size of the storage equipment.

TABLE 2. Selection of Salts and Alloys

Composition (weight percent)	Melting Point ^{o}C	Energy Storage Density, Solid (1) J/m^3	Thermal Conductivity Solid (2) $MJ/m \cdot sec. ^{o}C$	Raw Material Cost (3) \$/MJ	Relative Required Heat Transfer Area/MJ (4) m^2/MJ	Total cost (\$/MJ)
$NaNO_3$85.5, Na_2SO_4 8.8, NaCℓ5.7	278	385	0.78	0.81	29.6	4.23
$NaNO_3$95.4, NaCℓ4.6	297	403	0.69	0.83	30.7	4.08
$CaCℓ_2$69.9, NaCℓ30.1	490	558	4.0	0.29	10.8	1.50
KCℓ46.2, $CaCℓ_2$29.9, NaCℓ23.9	515	573	3.8	0.21	11.0	1.42
LiOH79, LiF21	427	1240	2.6	2.89	9.01	4.20
LiOH	460	1250	2.4	2.19	9.36	3.30
KF68, LiF32	492	1320	3.5	3.97	7.52	3.75
Aℓ67.75, Cu27.0, Si 5.25	524	1015	256	1.56	1.00	1.76
Aℓ66.8, Cu 33.2	548	965	273	1.73	1.00	1.94
Aℓ82.1, Si13.3, Mg 4.6	559	1100	199	1.11	1.09	1.29
Aℓ87.4, Si 12.6	577	1147	180	0.92	1.13	1.09

(1) Heats of fusion were calculated from $\Delta H_m = T_m \sum_i \frac{\Delta H_i X_i}{T_i}$. Densities were calculated from $\rho_m = \left[\sum_i \frac{X_i}{\rho_i}\right]^{-1}$ Accuracy is probably ±15%.

(2) Thermal conductivities were approximated from conductivities of pure components near the melting point of the eutectic or compound.

(3) Costs were based on costs per pound for technical grade salts or metal clippings from "Chemical Marketing and Drug Reporter" and "Iron Age".

(4) Relative areas are for a tubular heat exchanger configuration.

Storage systems using sensible heat utilize the solar energy collected to raise the temperature of the storage medium. The storage capacity is determined by the specific heat and the density of the material used. The most widely used materials for sensible heat storage are water and rock or gravel. The heat transfer calculations are fairly straightforward, and a typical sizing procedure is demonstrated below.

The heat transfer problem with change of phase, on the other hand, is nonlinear and has very few analytical solutions. For that reason, energy integral or numerical methods are usually utilized. The problem of phase change storage is complicated significantly due to the uncertainty about the following points: (a) Interface resistance between container walls and fluid. If the fluid does not wet the container, it may collect in the form of drops, reducing markedly the interface heat transfer area. (b) Interface resistance between walls and solid. (c) Determination of the extent of space to be left in the thermal storage container to accommodate the volume change associated with phase changes. Also, with large volume shrinkages (LiF, for example, shrinks to about 50%), void cavities arise in the frozen melt. These cavities, particularly if formed at heat transfer surfaces, will drastically affect the rate of heat transfer and introduce different mechanisms. Cavities forming on the heating elements (where present), would cause overheating and burn out of the elements. Some preliminary studies of void patterns [18] have shown that void patterns depend on the rate of heat transfer. Slow cooling of melts apparently causes large voids to occur, while rapid cooling seems to have an inhibiting effect. But with rapid cooling, new problems of thermal stress in the melt container arise. It is felt that ultimately extensive experimentation would be necessary before definitive conclusions can be drawn regarding the relationship between the rate of cooling and void formations. A further question is the void composition. Clearly, the nature of the contents will dictate the mode of heat transfer between the void boundaries. Complex natural convection currents or radiation or a combined mode may prevail. Depending on the mode, suitable mathematics has to be developed in order to evaluate the "actual" heat transfer rates. (d) Transmissivity of solid and liquid, at the operating temperatures, which is related to the relative effect of thermal radiation on the total heat transfer. (e) Radiative properties needed for (d) above are not available at present. (f) From the very nature of thermal storage, the transient aspects are of major importance, and the easier to solve steady state models would be inadequate.

With regard to sensible heat storage design, consider the following illustrative example. The storage is to be designed for a 100 MWe solar power station where the steam is produced by concentrated solar energy or by thermal storage material in the absence of sufficient (or any) sunshine. The superheated steam is to be expanded in a steam turbine with the steam admitted to the turbine (or to the thermal storage unit during charging) at the state of 500°C and 9×10^6 N/m^2. The turbine exhausts saturated steam at 20°C. The storage material is to be rock or gravel. The density, specific heat, and the equivalent diameter of gravel spheres are known to be 1536 kg /m^3, 754 J/kg°C, and 5 cm respectively. The expected "void" volume for the storage is about 42%. It is also expected

that the "nighttime" could be up to as much as 17 hours. We shall determine the size of the storage container, volume of the rock to be used, and the pressure drop for the system.

During charging, the entering superheated steam "sees" cold rocks and condensation would occur. With increasing time this "condensation-boundary" would move downward, and the rocks will get progressively hotter, until sufficient energy is stored. During discharge, cold water from the pump enters the storage and "sees" hot rocks. The liquid will evaporate and eventually leave the storage as superheated steam. As time goes on, this "evaporation-boundary" would move upward and the rocks will get progressively colder, until the necessary energy exchange has taken place. In this sense, the sensible heat storage problem involves a "mobile" boundary, although this is not the usual sense in which the terminology is used. At any given instant, during charging or discharging, there will be vapor and liquid flow regimes present so that essentially a three-zone model could be used to describe sensible heat storage in such a case.

Consider a packed storage of total height H that is divided into N equal layers of length Δx. Let the temperature gradients in directions transverse to that of the flow direction be negligible. Then, within a layer i, the storage material can be approximated as having a single uniform temperature $T_{b,i}$. For small to moderate values of the volumetric heat transfer coefficient, the fluid temperature will not be the same as the storage temperature, and as pointed out by Duffie and Beckman [25], it will be necessary to write two energy balances; one for the storage material and the other for the fluid. For the i^{th} bed layer, following Duffie and Beckman, an energy balance for storage heating (steam flow down during charging and flow up during discharging) yields

$$(PCA\Delta x)\frac{dT_{b,i}}{dt} = hA\Delta x(T_{f,i-1}-T_{b,i}) \qquad (1)$$

where A is the storage cross-sectional area, ρ is an apparent density, C is the specific heat of rock. The energy equation for the fluid becomes

$$\dot{m}C_p(T_{f,i-1}-T_{f,i}) = hA\Delta x(T_{f,i-1}-T_{b,i}) \qquad (2)$$

However, since the present problem concerns itself with a fluid that changes phase during charging and discharging, during the phase change process the latter equation needs to be replaced by

$$\dot{m}h_{fg}(\hat{x}_{f,i-1}-\hat{x}_{f,i}) = hA\Delta x(T_{f,i-1}-T_{b,i}) \qquad (3)$$

where x and h_{fg} are the quality and the latent heat (of vaporization during discharging or of condensation during charging), respectively.

It is important to note that when a single phase fluid (either vapor or liquid) is in contact with the storage material (either during charging or discharging), it is possible to determine an average heat transfer coefficient based on sensible heat transport calculations only. However, when a phase transformation occurs (either condensation or vaporization), the dependent variable for the fluid flow is the "quality" of the fluid instead of the temperature of the fluid. It is then the quality of the fluid that changes in the flow direction. The numerical solution procedure for the above set of equations therefore require monitoring the fluid temperature, along its flow path. When the fluid temperature is different from saturation, Eq. (3) is the proper one. Use of Eq. (3) is appropriate till the quality increases to unity value during discharging or decreases to zero for the charging process, at which point the controlling equation changes to Eq. (2). In this manner, the heat transfer coefficient and the corresponding storage dimensions can be determined. In the present illustration, instead of an exact solution of the set of these equations, a simplified method that can provide reasonable estimates for the storage size has been used. The pressure drop calculations are made using the Ergun [25] Equation:

$$\left(\frac{\Delta p\rho}{G^2}\right)\left(\frac{D}{H}\right)\left(\frac{\varepsilon^3}{1-\varepsilon}\right) = 150\,\frac{(1-\varepsilon)}{\left(\frac{DG}{\mu}\right)} + 1.75 \qquad (4)$$

where the maximum pressure drop corresponding to the end of the discharging period (the storage then will be filled with the liquid medium) is taken to be the appropriate value. The design pressure drop is obtained by adding the liquid hydrostatic head to the drop value as calculated from the Ergun Equation. The results for the sensible heat storage calculations for conditions given in Table III are given in Table IV.

Table III. Conditions for Sensible Heat Storage Calculations

Power Output of Plant = 100 MWe
Inlet Temperature for Charing = 500°C
Inlet Pressure of Steam = 9×10^6 N/m^2
Temperature of Water Entering Storage = 22°C
Turbine Efficiency = 0.9
Engine Efficiency = 0.9
Nighttime = 17 hours
Equivalent Diameter of Rock Pebbles = 5 cm

Table IV. Sizing of Sensible Heat Thermal Storage

Volume of Storage Required = 8.72×10^4 m^3
Size of Storage = 148 m x 148 m x 4 m
Height of Box for Storage = 4 m
Mass of Rock Required = 7.77×10^7 kg
Largest Pressure Drop in Storage System = 4×10^4 N/m^2

We next consider the storage design with a phase change material. The storage is to be designed for a 100 MWe solar power station where the steam is produced by concentrated solar energy or by the thermal storage material in the absence of sufficient (or any) sunshine. The superheated steam is to be expanded in a steam turbine with the steam admitted to the turbine (or to the thermal storage unit during charging) at the state of 566°C and 16.5×10^6 N/m^2. During operation from thermal storage, water is admitted in at 204°C, and the emerging steam is required to be at 482°C and at the specified maximum pressure given above. We select the phase change material to be Na_2SO_4-KCl-NaCl of weight percentages 57.6 - 40.4 - 2.0, respectively. The density, heat of fusion, and the melting point for the material are known to be 2345 kg/m^3, 514°C, and 181.3 kJ/kg, respectively. Using an iterative approach, we determine the transient and average heat transfer coefficients between the working fluid (water, steam) and the thermal storage material, the heat exchanger matrix and dimensions. We shall also identify the parameters of major importance to the problem.

The geometry of storage under consideration is shown in Fig.2. Assume a one-dimensional, constant property flow. Thus, $T_e(x)$ is the bulk average fluid temperature at any x. Consider N/2 slabs of phase change material (N half-slabs) each 2d thick, Y wide, and separated by a distance 2G. Neglect the thermal resistance of the containment material as well as density variations during fusion/melting.

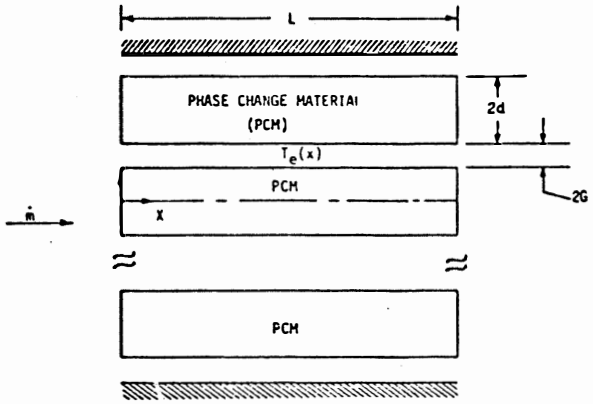

Fig. 2 Geometry for phase change storage

The slab can be assumed to initially contain all solid for the charging process and all liquid for the discharging process at the melting temperature (T_M). Consider the discharging process. At t = 0, cold fluid to be heated begins its flow over the slab, and the slab as it gives off heat begins to freeze. The downstream portions of the slab constantly see a higher temperature fluid since the fluid is heated as it flows along the slab. Consequently, the downstream portions freeze at a slower rate. Thus, a freezing front profile is established within the phase change material. As time progresses, more and more of the material is frozen and the front moves downstream.

With a neglect of conduction in the x and y directions, the energy equation in the solid is

$$\frac{\partial T}{\partial t} = \alpha \frac{\partial^2 T}{\partial z^2} \tag{5}$$

Consistent with the initial conditions, a uniform temperature (the melting temperature) exists within the liquid core. Thus, Eq. (5) is subject to the following boundary conditions:

$$T(z^*) = T_M \tag{6}$$

$$-k \left.\frac{\partial T}{\partial z}\right|_d = h(T(d)-T_e) \tag{7}$$

and

$$k \left.\frac{\partial T}{\partial z}\right|_{z^*} = \rho\lambda \frac{\partial z^*}{\partial t} \tag{8}$$

T_e appearing in Eq. (7) couples the energy equation of the phase change material with the energy equation for the externally flowing fluid, and this coupling can be established through a simple energy balance as

$$\rho_f C_f \left[\frac{\partial T_e}{\partial t} + V \frac{\partial T_e}{\partial x}\right] = \frac{h(T(d)-T_e)}{G} \tag{9}$$

subject to the boundary condition

$$T_e(x=0) = T_i \tag{10}$$

These equations can be nondimensionalized to yield

$$S \frac{\partial \theta}{\partial \tau} = \frac{\partial^2 \theta}{\partial \eta^2} \tag{11}$$

subject to

$$\theta(\eta^*) = 0 \tag{12}$$

$$-\left.\frac{\partial \theta}{\partial \eta}\right|_1 = B(\theta(1)-\theta_e) \tag{13}$$

$$-\left.\frac{\partial \theta}{\partial \eta}\right|_{\eta^*} = \frac{\partial \eta^*}{\partial \tau} \tag{14}$$

and

$$\gamma \frac{\partial \theta_e}{\partial \tau} + \frac{\partial \theta_e}{\partial \xi} = H(\theta(1)-\theta_e) \tag{15}$$

with

$$\theta_e(\xi=0) = 1 \tag{16}$$

where the variables are defined by

$$\theta = T_M-T/T_M-T_i,\ \theta_e = T_M-T_e/T_M-T_i,\ \eta = z/d,$$

$$\eta^* = z^*/d,\ \xi = x/L \text{ and, } \tau = t/(\rho\lambda d^2/k(T_M-T_i))$$

The parameters are defined by the Stefan number, S, Biot number, B, where

$$S = \frac{C(T_M-T_i)}{\lambda},\ B = \frac{hd}{k}, \text{ respectively}$$

and

$$\gamma = L/V/\rho\lambda d^2/k(T_M-T_i),\ H = \frac{YhL}{\dot{m}C_f}$$

The parameters γ and H are the ratio of the characteristic flow time to the characteristic freezing time, and the energy source strength per unit nondimensional temperature difference, respectively. Precisely the same equations govern the charging process so long as λ is considered to have a negative value and the material properties of the liquid are used.

The equations are solved under two limiting conditions. The first condition is that the Stefan number is zero. The error incurred by such an assumption is graphically displayed in Goodman [27] for the case of convective cooling-heating by a constant temperature fluid. There, the results indicate that this assumption leads to a maximum error of 10-20% in the prediction of the interface motion for the conditions assumed in the analysis. The second limiting condition is that γ is equal to zero. Since the characteristic flow times are of the order of seconds or minutes and the freezing times are of the order of hours, this should be a reasonable condition.

Numerous authors have considered problems similar to the one being considered here. Griggs, Pitts and Humphries [28], and Shamsundar and Sparrow [29, 30] considered the melting/freezing problem

with specialized boundary conditions, viz., constant heat flux and convection to a constant temperature fluid, respectively. Neither of these conditions is met in the actual heat exchanger since the heat flux and external temperature vary in the flow direction due to the coupling of the two energy equations. Yang and Lee [31] have made an attempt to solve this more general problem. However, they neglect the thermal resistance of the freezing solid or the melting liquid. Depending on the distance from the phase boundary to the wall and the thermal conductivity of the material, the temperature drop through this region can be quite significant. Matveev [32] derives an extremely simple solution to the problem, but his key assumptions lead to difficulties in applying his model to a design of the heat exchanger. Explicitly built into his model is the assumption that the flowing fluid exits the heat exchanger at the melting temperature of the phase change material and that the heat transfer coefficient is constant along the exchanger. Thus, it does not apply to a once through preheater/boiler/superheater since the heat transfer coefficient is not constant, nor to the individual components, which could be modeled as having a constant heat transfer coefficient, since the temperature exiting a given component does not necessarily correspond to the melting temperature.

Here we shall use an energy integral technique to solve Eqs. (11) through (16). Retaining linear terms in the $\theta(\eta)$ expansion, as suggested by Eq. (11) for S = 0, we have the following two governing equations

$$\frac{\partial \eta^*}{\partial \tau} = \theta_e/\eta^* - \left(\frac{1}{B} + 1\right) \qquad (17)$$

$$\frac{\partial \theta_e}{\partial \xi} = \frac{H}{B}\left[\theta_e/\eta^* - \left(\frac{1}{B} + 1\right)\right] \qquad (18)$$

with the initial condition for Eq. (17) given by

$$\eta^*(\tau=0) = 1.0$$

and the boundary condition for Eq. (18) given by Eq. (16). Clearly, the solution is of the form

$$\theta_e = \theta_e(\xi,\tau;\ H/B,\ B)$$

$$\eta^* = \eta^*(\xi,\tau;\ H/B,\ B)$$

These equations can now be solved via a finite difference formulation. Figure 3 shows $\eta^*(\xi,\tau)$ and $\theta_e(\xi,\tau)$ for typical values of B and H. The similar propagation of the phase boundary suggested by Matveev [32] is evident, but his assumption of a relatively short phase boundary development is not borne out. With a knowledge of $\eta^*(\xi,\tau)$ and $\theta_e(\xi,\tau)$, the local overall heat transfer coefficient U_ℓ can easily be determined. Figure 4 shows a nondimensional form of U_ℓ as a function of ξ and τ. Consistent with the previous assumptions, U_ℓ is only non-zero for $0 < \eta^* < 1$. As ξ increases, η^* increases, tending to increase U_ℓ, but at the same time θ_e is decreasing, which tends to decrease U_ℓ. The net result is that U_ℓ decreases as ξ increases for a given τ. For small τ and ξ, U_ℓ is relatively large. This is due to the fact that for small τ the phase boundary is not fully developed, and η^* can be relatively large without θ_e necessarily being small.

An instantaneous, spatially averaged heat transfer coefficient (U) can be found by integrating results of the form shown on Fig. 4. A nondimensional form of U is plotted versus τ in Fig. 5. An essentially constant value of Ud/k = 0.308 (for B = 25, H = 81) is observed up until the phase boundary reaches the exit plant ($\tau \cong 2.0$) at which time the performance begins to seriously deteriorate due to the decreasing area involved in the heat exchange. For small τ less area is also involved in the heat exchange, in comparison to that when the phase boundary is fully developed, but the higher U_ℓ's at low τ compensate for that effect.

This model for the heat transfer can now be used in the design of the storage system for the solar power plant. Based on the power output of the plant and the thermodynamic conditions of the working fluid, we determine the required mass flow rate through the turbine, which is also the mass flow rate through the thermal storage system during the discharge process. The average duration of discharging and charging processes is considered to be a known parameter. Through the use of the heat transfer analysis, the thermal storage system is designed such that the required mass flow rate is heated from the given inlet state to the given outlet state for the total discharging time period.

Next, the mass flow rate required to recharge storage system in the given charging time period is determined. The pressure drop in the system during charging and discharging are calculated. The results for the phase change heat storage calculations for conditions given in Table V are given in Table VI.

Table V. Conditions for Phase Change Storage Calculations

Power Output of Plant = 100 MWe
Inlet Temperature for Charging = 566°C
Power Cycle - Rankine (Maximum Pressure = 1.655×10^7 N/M^2)
Inlet Temperature for Discharging = 204°C
Outlet Temperature for Discharging = 482°C
Phase Change Material
Na_2SO_4 - kCl - NaCl of weights per cents
57.6 - 40.4 - 2.0
density = 2345 kg/m^3
melting point = 514°C
heat of fusion = 1.813×10^5 J/kg

Table VI. Sizing of Phase Change Thermal Storage (All Lengths in Meters)

Component	N	L	Y	d	G
Preheater	320	129.8	3.05	.0762	.00156
Boiler	680	148.7	1.52	.0762	.0127
Superheater	320	95.3	3.62	.0762	.00156

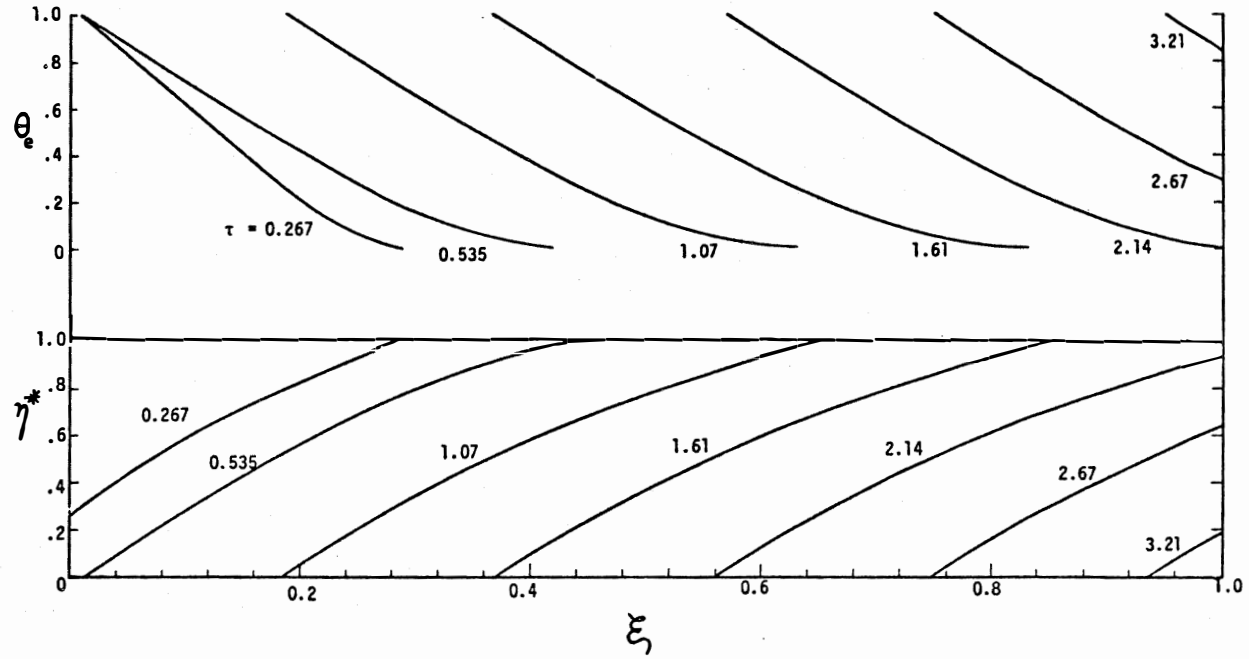

Figure 3. Temperature and phase boundary location vs. axial position (B = 25, H = 81, time is the plot parameter)

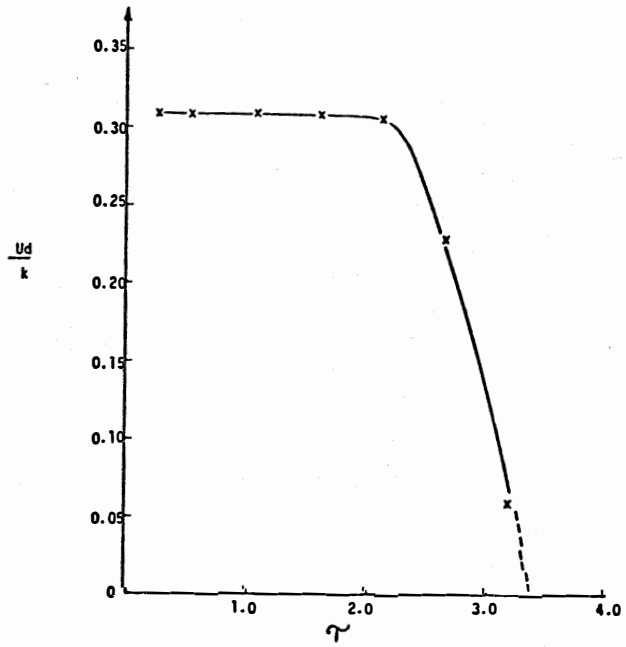

Figure 5. Spatially averaged heat transfer coefficient vs. time (B = 25, H = 81)

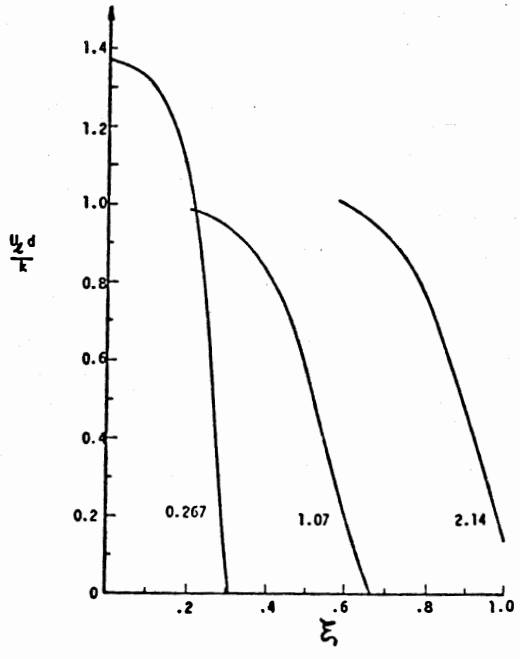

Figure 4. Overall heat transfer coefficient vs. axial location (B = 25, H = 81, time is the plot parameter)

CONCLUSIONS

Some properties of pure solid material relevant to thermal energy storage are generally available. Melting points, the nature of the transition (eutectic or peritectic - congruent or incongruent), heats of fusion, and solid phase densities, are often tabulated in easily available references. However, other important properties which are less available are the thermal conductivities and liquid densities near the melting point, from which the change in volume accompanying the phase change and the expansibility can be calculated. Research in the area of material property determination is strongly warranted.

With regard to the storage sizing, results presented here are of a preliminary nature, although all the relevant mathematical details have been developed and discussed in this paper. In particular, models presented in this paper reflect the state-of-the-art in transient analyses as appropriate to thermal storage calculations. A systematic numerical exploitation of the mathematical analyses presented here should yield reasonable results for thermal storage designs.

REFERENCES

[1] Martin Marietta Co., "Solar Power System and Component Research Program", Final Report, NSF/RANN/SE/AER/75-07570, Jan 1975.

[2] Fullman, R. L., "Energy Storage by Flywheels", Paper No. 759017, Proc. 10th IECEC, p. 91, Newark, DE, Aug 1975.

[3] Raetz, J. E., Easton, C. R. and Hall, R. J., "The Selection and Use of Energy Storage for Solar Thermal Electric Application", Paper No. 759088, Proc. 10th IECEC, p. 576, Newark, DE, Aug 1975.

[4] Yellott, J. I., "Power from Solar Energy", Trans. ASME, 1349 (1957).

[5] Athey, R. E., "Evaluation of the Flat Plate Solar Collector System for Electric Power Generation", Annual Meeting of the ISES (U.S. Section), Ft. Collins, CO, Aug 1974.

[6] Tabor, M., "Large Area Solar Collectors (Solar Ponds) for Power Production", U.N. Conf. on New Sources of Energy 4, Paper No. S/47, 59, Rome (1961).

[7] Dickinson, W. C., Clark, A. F., Day, J. A. and Wonters, L. F., "The Shallow Solar Pond Energy Conversion System", Solar Energy 18, 3 (1976).

[8] University of Minnesota and Honeywell, "Research Applied to Solar Thermal Power Systems", Progress Report No. NSF/RANN/SE/GI-34871/PR/72/4 (1972); 73/2 (1973); 73/4 (1974); 74/2 (1974); 74/4 (1975).

[9] Vant-Hull, L. L. and Hildebrand, A. F., "Solar Thermal Power System Based on Optical Transmission", Solar Energy 18, 31 (1976).

[10] Sabin, A., Wagner, W. and Easton, C. R., "Central Collector Solar Energy Receivers", Solar Energy 18, 21 (1976).

[11] Colorado State University and Westinghouse Electric Corp., "Solar Thermal Electric Power Systems" 3, Final Report No. NSF/RANN/SE/GI-37815/FR/74/3, Nov 1974.

[12] Goldstein, W., Steam Storage Installations, Pergamon Press, Oxford, 1970.

[13] Jones, T. B., Appendix C in Ref. [11].

[14] Telkes, M. and Raymond, E., "Storing Solar Heat in Chemicals - A Report on the Dover House", Heating and Ventilating, Vol. 46, pp. 80-86, (1949).

[15] Flynn, G. Jr., Percival, W. H. and Tsou, M., "Power from Thermal Energy Storage Systems", Society of Automotive Engineers, Paper #608B, 1962.

[16] Altman, M., "Prospects for Thermal Energy Storage", the 6th AGARD Colloquium on Energy Sources and Energy Conversion, Cannes, France, Mar 16-20, 1964.

[17] McKinnon, R. A., Vild, T. J. and Milko, J. A., "Design Study of Solar Brayton Cycle Cavity Receivers with Lithium Fluoride Heat Storage", AIAA Paper No. 64-727, Presented at the Third Biennial Aerospace Power Systems Conf., Phila, PA, Sept 1-4, 1964.

[18] Mattavi, J. N., Heffner, F. E. and Miklos, A. A., "The Stirling Engine for Underwater Vehicle Applications", Society of Automotive Engineers, Paper #690731, Oct 1969.

[19] Lorsch, H. G., Kauffman, K. W. and Denton, J. C., "Thermal Energy Storage for Heating and Off-Peak Air Conditioning", Energy Conversion 15, (1975).

[20] Ginen, D. M. and Sheft, I., "Metal Hydride Systems for Solar Energy Storage and Conversion", Proc. of NSF Workshop on Solar Energy Subsystems for the Heating and Cooling of Buildings", Report NSF-RA-N-75-041, Charlottesville, VA, 1975.

[21] Ervin, G., "Solar Heat Storage Based on Inorganic Chemical Reactions", Ibid.

[22] Goldstein, M., "Some Physical-Chemical Aspects of Heat Storage", U.N. Conf. on New Sources of Energy 5, Paper No. S/7, 411, Rome (1961).

[23] Schrenk, G. L. and Lior, N., "The Absorption Cycle Solar Heat Pump, and the Potential Role of Thermochemical Storage", Proc. ERDA Workshop on the Use of Solar Energy for the Cooling of Buildings, University of California, Los Angeles, Aug 4-6, 1975.

[24] Belton, G. and Ajami, F., "Thermochemistry of Salt Hydrates", Report No. NSF/RANN/SE/GI27976/TR/73/4, University of Pennsylvania, May 1973.

[25] Duffie, J. A. and Beckman, W. A., Solar Energy Thermal Processes, John Wiley & Sons, New York (1974).

[26] Ergun, S., "Fluid Flow through Packed Columns", Chem. Eng. Prog. 48, 89-94 (1952).

[27] Goodman, T. R., "The Heat-Balance Integral and Its Application to Problems Involving a Change of Phase", Trans ASME, Feb 1958.

[28] Griggs, E. A., Pitts, D. R., and Humphries, W. R., "Transient Analysis of a Thermal Storage Unit Involving a Phase Change Material", ASME Winter Annual Mtg., 1974, Heat Transfer Div.

[29] Shamsundar, N. and Sparrow, E. M., "Analysis of Multidimensional Conduction Phase Change Via the Enthalpy Model", J. Heat Transfer, Aug 1975.

[30] Shamsundar, N. and Sparrow, E. M., "Storage of Thermal Energy by Solid-Liquid Phase Change-Temperature Drop and Heat Flux", J. Heat Transfer, Nov 1974.

[31] Yang, W J. and Lee, C. P., "Dynamic Response of Solar Heat Storage Systems", ASME Winter Annual Mtg., 1974, Heat Transfer Div.

[32] Matveev, V. M., "Approximate Calculation of Heat Transfer in the Heat Storage System of a Solar Power Installation", Geliotekhnika 7, 5 (1971).

ERRATA FOR

"THERMAL ENERGY STORAGE CONSIDERATIONS FOR SOLAR-THERMAL POWER GENERATION"
(11th IECEC Paper No. 769107, September 1976)

by N. Lior, P. S. Ayyaswamy, J. O'Leary, K. W. Kauffman, H. Yeh, H. G. Lorsch

1. Subsequent to the work reported in this paper, it was found that the thermal properties used to calculate the thermal storage phase-change materials were in error. The calculation was repeated for the phase-change material KCl 46.2, $CaCl_2$ 29.9, NaCl 23.9. This is consistent with the results in Table 2 which show that this material has superior cost efficiency. The material properties used were

Density = 2159 kg/m^3

Heat of Fusion = 265.3 kJ/kg

Specific Heat = 840 J/kg m°C

Thermal Conductivity = 3.8 J/m sec°C

Melting Temperature = 515°C

The generalized heat transfer results were recalculated with new values of the non-dimensional parameters and are included in this addendum as Figures 3, 4, and 5 to replace the figures of the same numbers in the original paper.

The thermal storage system size was also recalculated. The design procedure remained the same. The three components of the system (preheater, boiler, superheater) were sized independently to meet their individual demands. The basic geometry of all three components is shown in Figure 2. The number of half-slabs, width of the half-slabs, and thickness of the half-slabs were somewhat arbitrarily assumed, but with optimization of heat transfer and pressure drop in mind. With these parameters fixed, the heat transfer analysis was used to determine the length of slabs required to heat the fluid by the required amount during a given period of time. On the one hand, an increase in slab length results in an increase in the length of time for which a given set of slabs lasts, thus resulting in a decrease in the number of sets required to last for the entire discharge period. On the other hand, however, longer slabs pose pressure drop and charging difficulties. A reasonable heat discharge time period for a set of slabs was assumed to be one hour, i.e., the total flow through the heat exchanger would be directed sequentially through a number of sets of slabs, each set receiving the flow for one hour. The heat transfer analysis was also used to determine the mass flow rate required to charge the entire system during the available time period (assumed to be 7 hours). The results are given in the Table VI below (which is to replace the table of the same number in the original paper).

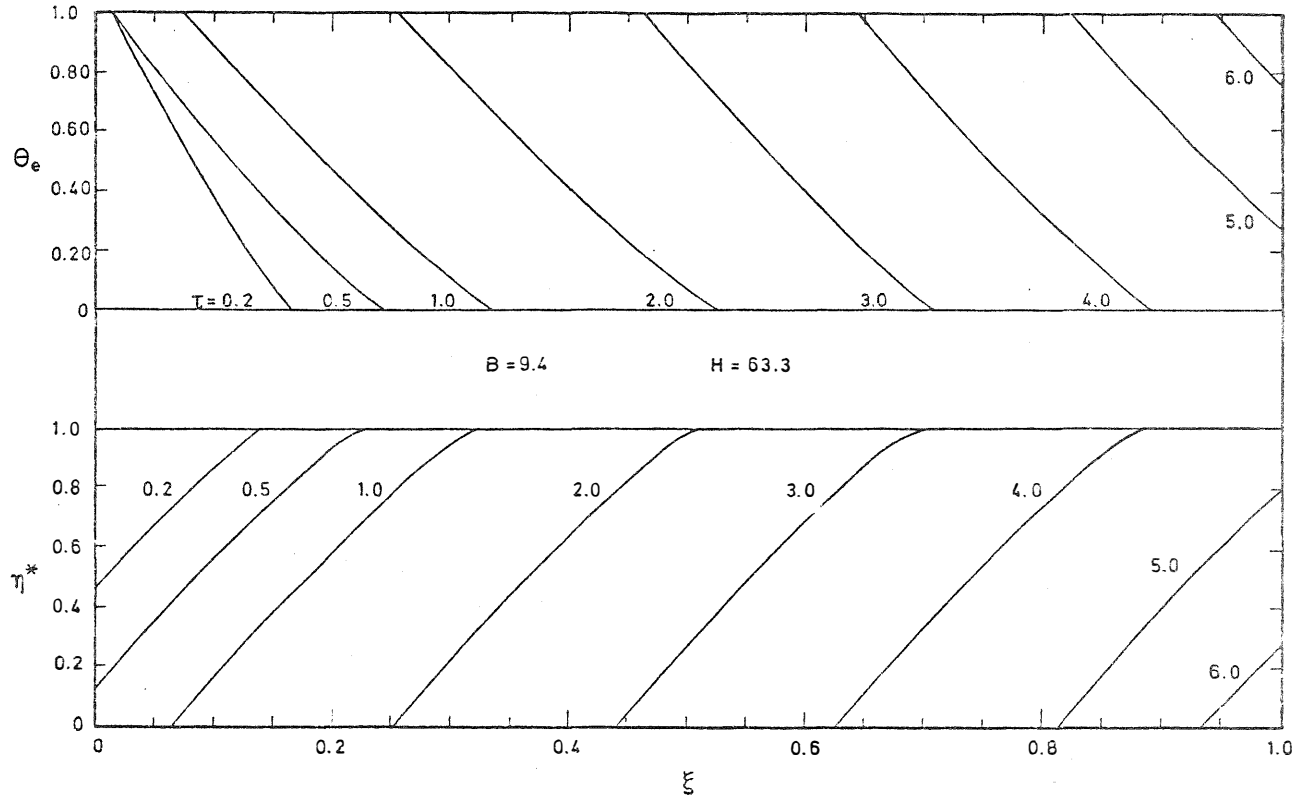

Figure 3. Temperature and Phase Boundary Location vs. Axial Position

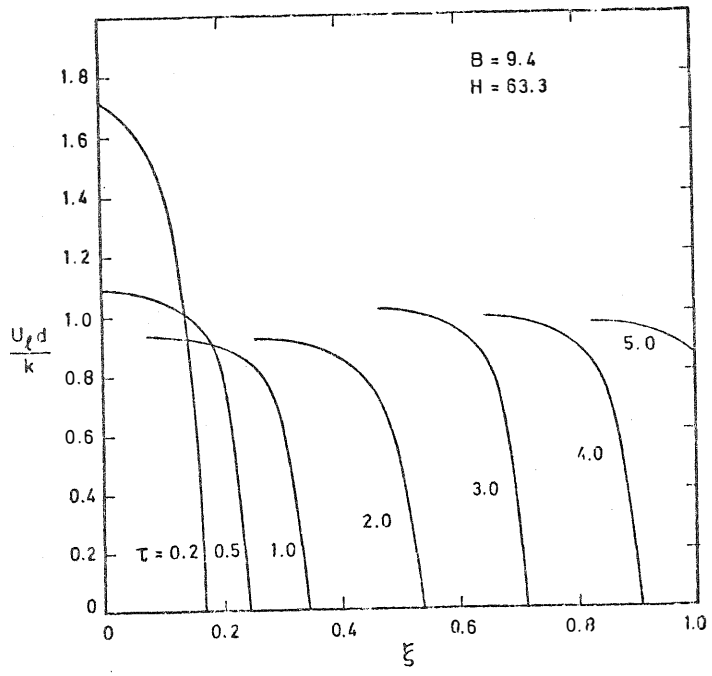

Figure 4. Overall Heat Transfer Coefficient vs. Axial Position

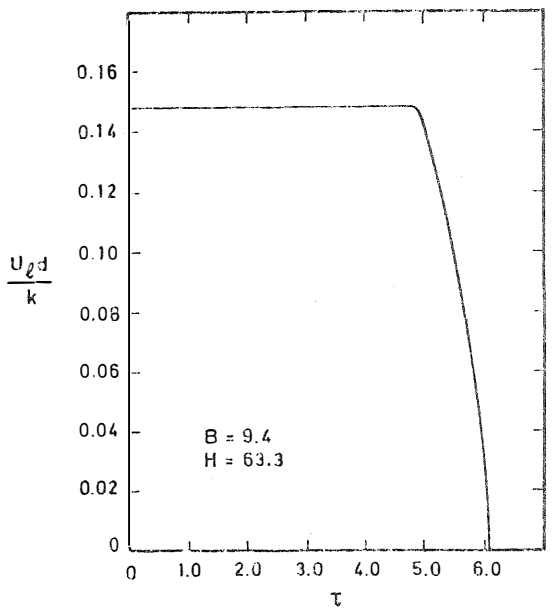

Figure 5. Spatially Averaged Heat Transfer Coefficient vs. Time

TABLE VI. Sizing of Phase Change Thermal Storage

Mass Flow Rate to Change = 1.34×10^7 kg/hr

	N	L,[m]	Y,[m]	d,[m]	G,[m]	$\Delta P[N/m^2]$
Preheater	374	84.9	6.1	0.0381	0.00435	1,700
Boiler	374	96.5	6.1	0.0381	0.00435	1,700
Superheater	374	78.1	6.1	0.0381	0.00435	14,000

Volume of Storage Required = 2.26×10^4 m^3

Mass of TES Material Required = 4.87×10^7 kg

OTHER ERRORS

	page	column	line	reads	should read
2.	2	left	21 from bottom	[3,8,10]	[3,9,10]
3.	3	left	15 from top	"in the absorption"	"in absorption"
4.	3	right	27 from bottom	14°C	60°C
5.	3	right	25 from bottom	$53.8/$m^2$	$55/$m^2$
6.	4	Table II	4 from top	J/m^3 MJ/m sec°C	MJ/m^3 J/m sec°C
7.	4	left	12 from bottom	50%	25%
8.	5	right	15 from top	[25]	[26]
9.	5	right	29 from top	Charing	Charging
10.	5	right	33 from top	Engine	Generator
11.	9	left	Ref. [6]	Tabor, M.	Tabor, H.
12.	9	left	Ref. [7]	Wonters	Wouters
13.	9	left	Ref. [10]	Sabin	Sobin
14.	9	right	Ref. [12]	Goldstein	Goldstern
15.	9	right	Ref. [20]	Ginen	Gruen